J|A|C|S
COMMUNICATIONS

Published on Web 02/26/2005

Wafer-Scale Periodic Nanohole Arrays Templated from Two-Dimensional Nonclose-Packed Colloidal Crystals

Peng Jiang*,† and Michael J. McFarland

Corning Science and Technology, Corning Incorporated, Corning, New York 14831

Received November 30, 2004; E-mail: pjiang@princeton.edu

Since the discovery of surface-plasmon-assisted extraordinary optical transmission,[1] periodic metal nanohole arrays have attracted great interest because of their important technological applications in nanophotonic devices (e.g., miniaturized optical waveguides, switches, and couplers),[2−4] information storage,[5,6] solar cells,[7] near-field scanning optical microscopy,[5] surface-enhanced Raman spectroscopy (SERS),[8] and biosensors.[9] To fabricate subwavelength hole arrays, electron beam lithography[4] and focused-ion-beam milling[1] are commonly used. However, these processes are expensive and tend to be limited by their low throughput. Here we report a much simpler and cheaper nonlithographic approach for fabricating wafer-scale periodic nanohole arrays by using two-dimensional nonclose-packed colloidal crystals as templates.

Two-dimensional (2D) close-packed colloidal crystals have been widely explored as sacrificial templates in creating regular arrays of nanopatterns.[10] In nanosphere lithography (NSL), a monolayer or double-layer colloidal crystal is used as either an etching or deposition mask to define a mosaic array of microcolumnar structures inside the voids of colloids.[11] Metallic and ceramic through-pore arrays have been made by electrochemical and sol−gel deposition through templates of 2D colloidal crystals.[12,13] As colloids are densely packed in the templates, the resultant spherical pores are interconnected, and multiple steps are required to make isolated nanohole arrays for subwavelength optics.[12] Additionally, although these self-assembly approaches are favorable for laboratory-scale production, their scaling-up are problematic as they are not compatible with standard microfabrication techniques that have been widely used in microelectronic and photonic industries.

We adapted our recently developed spin-coating technique in creating 2D nonclose-packed colloidal crystals as templates.[14,15] Similar to the formation of 3D colloidal crystals, we believe the normal pressures produced by spin-coating and monomer photopolymerization squeeze particles against the substrates to form nonclose-packed 2D crystals.[14,15] Figure 1 shows a typical scanning electron microscope (SEM) image of a 2D nonclose-packed colloidal crystal consisting of silica particles of 320 nm diameter. The long-range hexagonal ordering is evident from the image and is further confirmed by the fast-Fourier transform (FFT) of a 40 μm × 40 μm region shown in the bottom inset of Figure 1. From the more highly magnified image (upper inset), it is clearly seen that particles are not touching each other but exhibit center-to-center distance around 1.4D, where D is the diameter of colloids.[14] Although there are defects in the spin-coated 2D colloidal crystal, such as point defects and grain boundaries, the resulting colloidal monolayer with uniform interparticle distance covers the entire wafer area.[15]

A schematic outline of the procedures for templating isolated nanohole arrays from 2D nonclose-packed colloidal crystals is shown in Figure S1. Conventional physical vapor deposition (PVD) techniques, such as RF and DC-magnetron sputtering, thermal evaporation, and electron beam evaporation, are used to deposit a thin layer of material (10−100 nm) through the colloidal crystal templates. The spheres function as shadow masks to obstruct material deposition underneath them. As the colloids are not in contact in the original templates (see Figure 1), the deposited materials fill interstitials to form continuous films rather than distinct islands as in nanosphere lithography.[11] After removing colloids by brief ultrasonication in water or by simply sweeping using a cleanroom Q-tip under flowing water, wafer-scale periodic nanohole arrays can be made. As there is no need for using harsh chemicals to wet-etch silica colloids, a large variety of functional materials, ranging from metals (e.g., Au, Ag, Pt, Pd, Ti, Cr) to semiconductors (ITO, Ge, Si) and dielectrics (silica), can be used to create large-area periodic nanohole arrays.

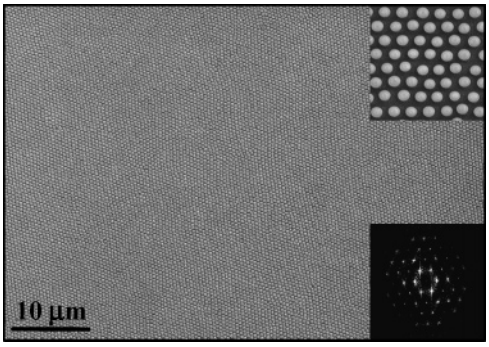

Figure 1. Typical SEM image of a 2D nonclose-packed silica colloidal crystal. The upper inset showing a higher-magnification image and the bottom inset showing a Fourier transform of a 40 μm × 40 μm region.

Figure 2A shows a photo of a 30-nm-thick chromium nanohole array templated from 320-nm diameter particles on a 4-in. (81 cm^2) silicon wafer. Under white-light illumination, the sample exhibits characteristic six-arm diffraction with exact 60° angles between adjacent arms, which indicates hexagonal ordering of nanoholes over the entire sample surface.[14,16] The different reflected colors are caused by different incident angles of the illuminating white light. The long-range hexagonal ordering of the sample is clearly evident from the SEM image and the FFT shown in Figure 2B and its inset. The SEM image also reveals that the nanoholes match the size of the template spheres and retain their center-to-center distance (∼1.4D).

To make practical subwavelength optical devices, such as optical waveguides and couplers, patterning of metal nanohole arrays with micrometer-scale resolution is important.[2] Because of the on-wafer planar configuration and the uniform monolayer coverage of the colloidal crystal templates, complex micropatterns with submicrometer resolution can be easily made by standard photolithography. Figure 2C shows a SEM image of a micropatterned chromium nanohole array templated from 320-nm silica spheres. The higher-magnification image (Figure 2D) reveals the good

† Present address: Department of Chemical Engineering, Princeton University, Princeton, NJ 08544.

10.1021/ja042789+ CCC: $30.25

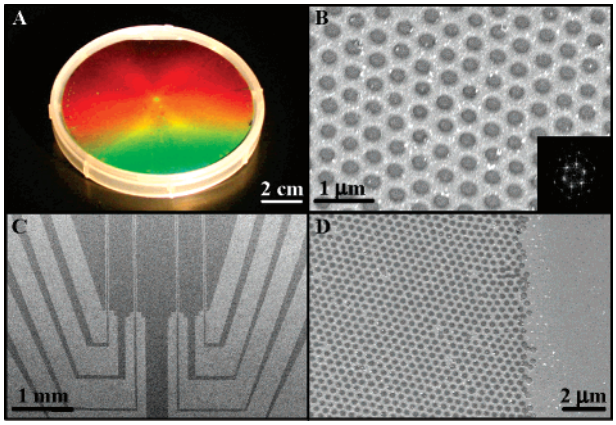

Figure 2. (A) Photograph of a 30-nm-thick chromium nanohole array on a 4-in. silicon wafer illuminated with white light. (B) Typical top-view SEM image and its FFT of the sample shown in (A). (C) SEM image of a micropatterned nanohole array. (D) Higher magnification SEM image of (C). Chromium was deposited by a Denton DV-502A E-beam evaporator.

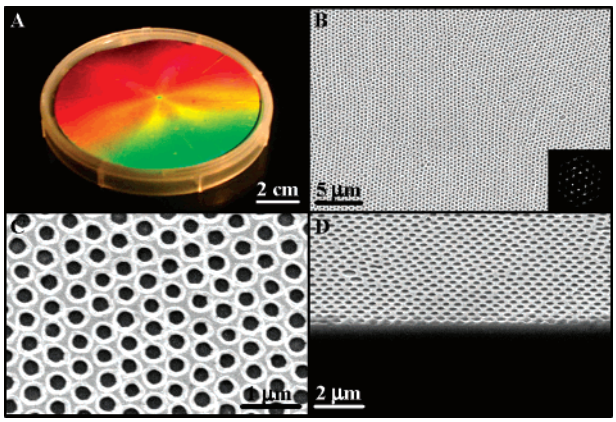

Figure 3. (A) Photograph of a 4-in.-diameter silicon nanohole array made by the double-template approach. (B) Typical top-view SEM image and its FFT (inset) of the sample shown in (A). (C) Magnified SEM image. (D) Side-view SEM image.

definition of the lithographic patterning. It is also clearly seen that the long-range ordering and the center-to-center spacing of the colloidal crystal templates are well preserved during the entire patterning process.

The templated nanohole arrays can be used as second-generation etching masks to transfer the periodic circular holes to the substrates underneath by using conventional reactive ion etching (RIE) (see Figure S1). Figure 3A shows a photo of a doubly templated regular void array on a 4-in. silicon wafer; 30-nm-thick chromium nanohole arrays templated from 320-nm silica spheres are used as the etching mask. RIE using SF_6 is then applied to etch the silicon substrate, underneath. After dissolving chromium in CR-7 etchant (Transene), the resultant silicon sample exhibits stronger reflectivity than the templating metal nanohole array due to less optical absorption. The striking six-arm diffraction shown in Figure 3A and the typical SEM and FFT of the sample shown in Figure 3B demonstrate the long-range hexagonal ordering of the submicrometer voids. These voids keep the arrangement and the center-to-center distance of the original silica colloidal crystal as revealed by the magnified SEM image in Figure 3C. However, the size of the silicon voids appears larger than that of silica spheres and chromium nanoholes due to the isotropic etching during the SF_6 RIE process. This can be confirmed by the slanted sidewalls of the voids as shown by the side-view SEM image in Figure 3D. The etching depth of the voids can be easily controlled by adjusting the etching conditions (e.g., power, gas composition and pressure, and time). Although we only use silicon as the substrate here, the double-template approach can be generalized to other functional substrates, such as GaAs, InP, and glass, to fabricate wafer-scale periodic void arrays that may have important technological applications ranging from 2D photonic crystals[17] to interferometric biosensors.[18]

In summary, we have developed a simple yet versatile nonlithographic approach for mass-fabricating wafer-scale periodic nanohole arrays from a large variety of functional materials, including metals, semiconductors, and dielectrics. Complex micropatterns can be created by standard microfabrication for potential device applications.

Supporting Information Available: Scheme of the double-template fabrication process and experimental procedures. This material is available free of charge via the Internet at http://pubs.acs.org.

References

(1) Ebbesen, T. W.; Lezec, H. J.; Ghaemi, H. F.; Thio, T.; Wolff, P. A. *Nature* **1998**, *391*, 667−669.
(2) Barnes, W. L.; Dereux, A.; Ebbesen, T. W. *Nature* **2003**, *424*, 824−830.
(3) Hutter, E.; Fendler, J. H. *Adv. Mater.* **2004**, *16*, 1685. Andrew, P.; Barnes, W. L. *Science* **2004**, *306*, 1002−1005.
(4) Altewischer, E.; van Exter, M. P.; Woerdman, J. P. *Nature* **2002**, *418*, 304−306.
(5) Thio, T.; Lezec, H. J.; Ebbesen, T. W.; Pellerin, K. M.; Lewen, G. D.; Nahata, A.; Linke, R. A. *Nanotechnology* **2002**, *13*, 429−432.
(6) Jenkins, D.; Clegg, W.; Windmill, J.; Edmund, S.; Davey, P.; Newman, D.; Wright, C. D.; Loze, M.; Armand, M.; Atkinson, R.; Hendren, B.; Nutter, P. *Microsyst. Technol.* **2003**, *10*, 66−75.
(7) Westphalen, M.; Kreibig, U.; Rostalski, J.; Luth, H.; Meissner, D. *Sol. Energy Mater. Sol. Cells* **2000**, *61*, 97−105.
(8) Tessier, P. M.; Velev, O. D.; Kalambur, A. T.; Rabolt, J. F.; Lenhoff, A. M.; Kaler, E. W. *J. Am. Chem. Soc.* **2000**, *122*, 9554−9555.
(9) Homola, J.; Yee, S. S.; Gauglitz, G. *Sens. Actuators B* **1999**, *54*, 3−15.
(10) (a) McLellan, J. M.; Geissler, M.; Xia, Y. N. *J. Am. Chem. Soc.* **2004**, *126*, 10830−10831. (b) Barton, J. E.; Odom, T. W. *Nano Lett.* **2004**, *4*, 1525−1528. (c) Choi, D. G.; Yu, H. K.; Jang, S. G.; Yang, S. M. *J. Am. Chem. Soc.* **2004**, *126*, 7019−7025. (d) Choi, D. G.; Kim, S.; Jang, S. G.; Yang, S. M.; Jeong, J. R.; Shin, S. C. *Chem. Mater.* **2004**, *16*, 4208−4211. (e) Jiang, P. *Angew. Chem., Int. Ed.* **2004**, *43*, 5625−5628. (f) Hakanson, U.; Persson, J.; Persson, F.; Svensson, H.; Montelius, L.; Johansson, M. K. J. *Nanotechnology* **2003**, *14*, 675−679. (g) Lu, Y.; Xiong, H.; Jiang X.; Xia, Y. N.; Prentiss, M.; Whitesides, G. M. *J. Am. Chem. Soc.* **2003**, *125*, 12724−12725.
(11) (a) Deckman, H. W.; Dunsmuir, J. H. *Appl. Phys. Lett.* **1982**, *41*, 377−379. (b) Haynes, C. L.; Van Duyne, R. P. *J. Phys. Chem. B* **2001**, *105*, 5599−5611.
(12) Abdelsalam, M. E.; Bartlett, P. N.; Baumberg, J. J.; Coyle, S. *Adv. Mater.* **2004**, *16*, 90−93.
(13) (a) Sun, F. Q.; Cai, W. P.; Li, Y.; Cao, B. Q.; Lei, Y.; Zhang, L. D. *Adv. Funct. Mater.* **2004**, *14*, 283−288. (b) Wang, X. D.; Graugnard, E.; King, J. S.; Wang, Z. L.; Summers, C. J. *Nano Lett.* **2004**, *4*, 2223−2226.
(14) Jiang, P.; McFarland, M. J. *J. Am. Chem. Soc.* **2004**, *126*, 13778−13786.
(15) Jiang, P.; Prasad, T.; McFarland, M. J.; Colvin, V. L. Manuscript in preparation.
(16) Hoffman, R. L. *Trans. Soc. Rheol.* **1972**, *16*, 155−165.
(17) Birner, A.; Wehrspohn, R. B.; Gosele, U. M.; Busch, K. *Adv. Mater.* **2001**, *13*, 377−388.
(18) Lin, V. S. Y.; Motesharei, K.; Dancil, K. P. S.; Sailor, M. J.; Ghadiri, M. R. *Science* **1997**, *278*, 840−843.

JA042789+